Rare Metal Materials and Engineering
Volume 45, Issue 5, May 2016
Online English edition of the Chinese language journal

Available online at www.sciencedirect.com
ScienceDirect

Cite this article as: Rare Metal Materials and Engineering, 2016, 45(5): 1117-1121.

ARTICLE

High Visible-light Photocatalytic Activity of γ-Fe_2O_3/TiO_2 Nanotube Heterojunction Arrays

Zhou Guanghong[1,2], Ding Hongyan[1], Zhu Yufu[1], Lin Yuebin[1], Liu Peng[2]

[1] Jiangsu Provincial Key Laboratory of Interventional Medical Devices, Huaiyin Institute of Technology, Huaian 223003 China; [2] School of Physical and Mathematical Sciences, Nanyang Technological University, Singapore 637371

Abstract: This study presents the preparation and the application of γ-Fe_2O_3/TiO_2 nanotube magnetic heterojunction photocatalysts (MHPs) for photodegradation of methylene blue under visible light irradiation. The morphology, the microstructure, the magnetic properties and the photocatalytic activity of γ-Fe_2O_3/$TiO_{2\,(NT)}$ MHPs were studied. Results show that the MHPs are provided with highly ordered TiO_2 (titania) nanotube arrays (55 nm in diameter and 10 nm in wall thickness) and nano γ-Fe_2O_3 (maghemite) particle (approximately 15 nm) co-deposition. The MHPs exhibit a superparamagnetic behavior of γ-Fe_2O_3/$TiO_{2\,(NT)}$ MHPs resulting from the small size of γ-Fe_2O_3 particles. The photocatalytic activity of γ-Fe_2O_3/$TiO_{2\,(NT)}$ MHPs is greater than that of Fe_3O_4/$TiO_{2\,(NT)}$ MHPs or pure $TiO_{2\,(NT)}$ under visible light irradiation. The interaction between γ-Fe_2O_3 and TiO_2 improves charge separation and extends TiO_2 response into the visible region. Moreover, the formed heterojunction between γ-Fe_2O_3 and TiO_2 can further prevent the recombination between photoelectrons and holes.

Key words: visible-light; photocatalytic; nanotube; heterojunction arrays; magnetic

Semiconductor photocatalysts have attracted extensive attention since the past three decades. Among these photocatalysts, TiO_2 has become the most promising material because it is inexpensive and exhibits high photocatalytic activity, chemical stability and non-toxic properties[1]. TiO_2 can generate electron-hole pairs (e^-/h^+) after UV radiation (λ<385 nm), which induces a series of reactions to generate free-radicals that are very efficient oxidizers of adsorbed pollutants[2]. Unfortunately, only about 5% of the total irradiated natural sunlight has sufficient energy to cause efficacious photocatalysis[3,4]. Therefore, it is necessary to develop effective solutions to improve charge separation efficiency and visible-light photoactivity. TiO_2 nanotubes exhibit better photocatalytic ability because of the large specific surface area of their tubes and more production of e^-/h^+ pairs upon light irradiation[5,6]. TiO_2 nanotubes have recently been widely applied in dye-sensitized solar cells[7], biomedical applications[8] and detection sensors[9].

One-dimensional heteronanostructures exhibit enhanced properties because of two kinds of functional materials and the formation of heterojunctions at the interface[10]. A well-established heterojunction structure could be employed to increase the lifetime of charge carriers and enhance the quantum yield. Ferroferric oxide (Fe_3O_4) nanoparticles, a semiconductor, possess better light harvesting and charge transport properties. TiO_2/Fe_3O_4 magnetic photocatalysts have already been tested for photodegradation of water pollutants, phenol and dyes in most of the cases[11-13]. However, Beydoun et al revealed that the TiO_2/Fe_3O_4 composite photocatalyst did not exhibit high photocatalytic ability as expected, instead of photocatalytic ability lower than that of single-phase TiO_2[12]. This finding was attributed to an unfavorable heterojunction between TiO_2 and Fe_3O_4; that is, the photogenerated electrons elevated to the conduction band of the TiO_2 nanocrystals were injected into the lower lying conduction band of the Fe_3O_4 core, thereby increasing the electron-hole recombination.

The heterojunction structure between TiO_2 nanotubes and γ-Fe_2O_3 with matched band potentials may provide an

Received date: May 25, 2015
Foundation item: Nature Science Foundation of Jiangsu Province (BK2012668); Qinglan Project of Jiangsu Higher School (2014)
Corresponding author: Ding Hongyan, Ph. D., Professor, Jiangsu Provincial Key Laboratory of Interventional Medical Devices, Huaiyin Institute of Technology, Huaian 223003, P. R. China, Tel: 0086-517-83559130, E-mail: nanhang1227@gmail.com

effective way to improve photocatalytic activity. Given that the band gap (E_g) of γ-Fe_2O_3 is only 2.2 eV, more visible light can be absorbed and more electrons are generated. Thus, the electrons excited by the visible light can be transferred to TiO_2 from γ-Fe_2O_3, which favors the charge separation and improves the visible-light photocatalytic activity of the heterostructure dramatically[14-16].

In the present study, a simple way of preparing magnetic γ-Fe_2O_3 nanoparticles deposited on TiO_2 nanotubes, namely, MHPs, was described. This composite material took full advantage of the TiO_2 nanotubes with higher specific surface area and the γ-Fe_2O_3 nanoparticles with good visible-light absorption properties in photocatalysis. The photocatalytic activity of MHPs was studied through photodegradation of methylene blue (MB) in wastewater because MB is difficult to remove in wastewater from the textile industry.

1 Experiment

Titanium (Ti) foils (20 mm×40 mm×0.6 mm) were mechanically polished using different grades of sandpapers, followed by ultrasonic cleaning in isopropanol and water. The foils were then ultrasonically cleaned in acetone and rinsed with deionized water. Hydroxide islands were created by dipping the polished Ti foil in an acidic solution containing 1 wt% H_3PO_4 and 0.1 wt% HF for 2 min, followed by sonicating in deionized water for 5 min. H_3PO_4 was used to adjust the solution pH to 1.5, whereas F^- was used to initialize the formation of a hydroxide layer.

Anodization was performed in an electrochemical cell using a platinum plate as the cathode. The electrolyte contained 0.25 wt% NH_4F and 1 wt% water in ethylene glycol. The anodizing voltage was kept constant at 20 V DC with a fixed electrode separation of 40 mm. The surface area exposed to the electrolyte was about 1600 mm^2 (800 mm^2 each side). The experiments were performed at 25 ℃ for 2 h.

Up to 20 mL of 0.2 mol/L $FeCl_3$ solution was mixed with 20 mL of 0.1 mol/L $FeCl_2$ solution in a flask. The as-prepared TiO_2 nanotube specimens were added into the mixed solution with ultrasonic oscillation for 5 min, followed by slow addition of 80 mL of 25 wt% $NH_3 \cdot H_2O$ solution, with vigorous stirring. The reaction was maintained for 2 h and the solution color changed from orange to black, indicating the generation of Fe_3O_4.

Finally, the deposited specimens were washed with deionized water three times to remove the unreacted chemicals. The deposited specimens were then annealed at 400 ℃ for 2 h in air and nitrogen separately for further investigation. Fe_3O_4 was transformed into γ-Fe_2O_3 after calcination at high temperature in air, but remained untransformed in nitrogen.

X-ray diffraction patterns were collected on a diffractometer (XRD) with Cu Kα radiation. The morphology and the size of the MHPs were characterized by field emission scanning electron microscopy (FESEM). Magnetic measurements were carried out at room temperature using a physical property measurement system (PPMS) with VSM magnetometer.

Photocatalytic activities of the MHPs were studied by degradation of MB in a self-made photocatalytic reactor. The sunlight was used as light source; an air-blowing apparatus was also used. The modulated wastewater was prepared by dropping MB into deionized water. The content of MB in the modulated water was about 10 mg/L. Air was continuously supplied to the system at a flow rate of 50 L/h to keep the concentration of dissolved oxygen near its saturation. The γ-Fe_2O_3/$TiO_{2\,(NT)}$ and Fe_3O_4/$TiO_{2\,(NT)}$ MHPs were added in the modulated water with the amount of 1600 mm^2/L, respectively. TiO_2 nanotubes annealed at 400 ℃ for 2 h in air without deposition of any magnetic nanoparticles were also added in the modulated water under the same conditions for comparison. To determine the change of MB concentration during the photocatalytic process, a few milliliters of solution were taken out from the mixture various times, and then measured with UV-Vis spectrometer (UV-2802PC Unico). The degradation ratio of MB was calculated from the absorbance at 660 nm, using the following formula:

$$R = (C_0 - C)/C_0 \times 100\% \quad (1)$$

where R is the degradation ratio; C_0 is the initial absorbance; C is the absorbance of the solution at various times.

2 Results and Discussion

2.1 XRD studies

Fig.1 shows the XRD patterns of the MHPs with γ-Fe_2O_3 and Fe_3O_4. No obvious difference was observed between the two patterns. This result can be explained by the following two reasons. The main reason is that the crystal structure of Fe_3O_4 and γ-Fe_2O_3 are similar, i.e., their peak shapes and positions are very close; hence, XRD analysis cannot provide enough evidence for confirmation[17,18]. The other reason is that the amount of Fe_3O_4 or γ-Fe_2O_3 is little, only about 5 wt% according to the quantitative analysis. Thus, although differences exist in the intensity of patterns, they can be considered negligible compared with those of Ti and TiO_2. A previous study reported that Fe_3O_4 and γ-Fe_2O_3 can be discerned using the X-ray photoelectron spectroscopy technique, e.g., Fe $2p_{3/2}$ and Fe $2p_{1/2}$ are 710.35 and 724.0 eV for γ-Fe_2O_3 and 711.29 and 724.82 eV for Fe_3O_4 [19]. However, Fe_3O_4 and γ-Fe_2O_3 can be distinguished by simply measuring their saturation magnetic moments, which will be discussed in section 2.3.

Fig.1a and 1b show that all the peaks are assigned to those of hexagonal Ti with diffraction peaks at 2θ = 35.17°, 38.45°, 40.25°, and 53.09° and anatase TiO_2 with diffraction peaks at 2θ=25.30°, 37.79°, 48.05°, and 53.88° (JCPDS Card No. 71-1166, 89-5009, 19-0629 and 39-1346). No diffraction peak was observed from the impurities, suggesting the high phase purity of the heterojunction arrays.

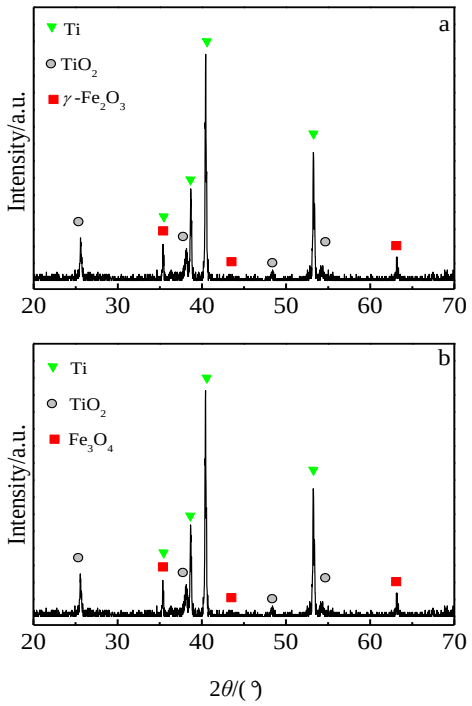

Fig.1 XRD patterns of the MHPs: (a) γ-Fe_2O_3/$TiO_{2\,(NT)}$ MHPs and (b) Fe_3O_4/$TiO_{2\,(NT)}$ MHPs

In addition, the mean size (D) of a single γ-Fe_2O_3 crystallite can be determined from the full-width at half-maximum (FWHM) of a corresponding X-ray diffraction peak using Scherrer's formula $D=k\lambda/(\beta\cos\theta)$[20], where λ is the wavelength of the X-ray radiation (λ=0.154 18 nm), k is the Scherrer constant (k=0.9), θ is the appropriate X-ray diffraction angle, and β is the FWHM. The estimated nanocrystallite size of γ-Fe_2O_3 is 5.4 nm, which can be calculated; the grain size of Fe_3O_4 is approximately 5.2 nm.

2.2 Morphology studies

Fig.2a presents the morphology of highly ordered TiO_2 nanotube arrays grown on the Ti foils. The inset of Fig.2a indicates that the TiO_2 layer consists of nanotube arrays with an average nanotube diameter of 55 nm and wall thickness of about 10 nm. Fig.2b shows an SEM image of the surface of γ-Fe_2O_3/$TiO_{2(NT)}$ MHPs. A narrow-sized distribution of γ-Fe_2O_3 nanoparticles can be clearly observed. The morphology and the structural integrity of the TiO_2 nanotube arrays remain unaltered after γ-Fe_2O_3 loading. The figures clearly show that the γ-Fe_2O_3 nanoparticles are distributed on the surfaces of TiO_2 nanotubes with a few aggregations, whereas the sizes of the γ-Fe_2O_3 nanoparticles are about 15 nm to 25 nm. The γ-Fe_2O_3 particle size shown by FESEM is much larger than that calculated by XRD because FESEM shows agglomeration of the particles, whereas XRD provides an average crystallite size. The XRD and FESEM data can be reconciled by the fact that smaller primary particles have large surface free energy and would thus tend to agglomerate faster and grow into larger grains.

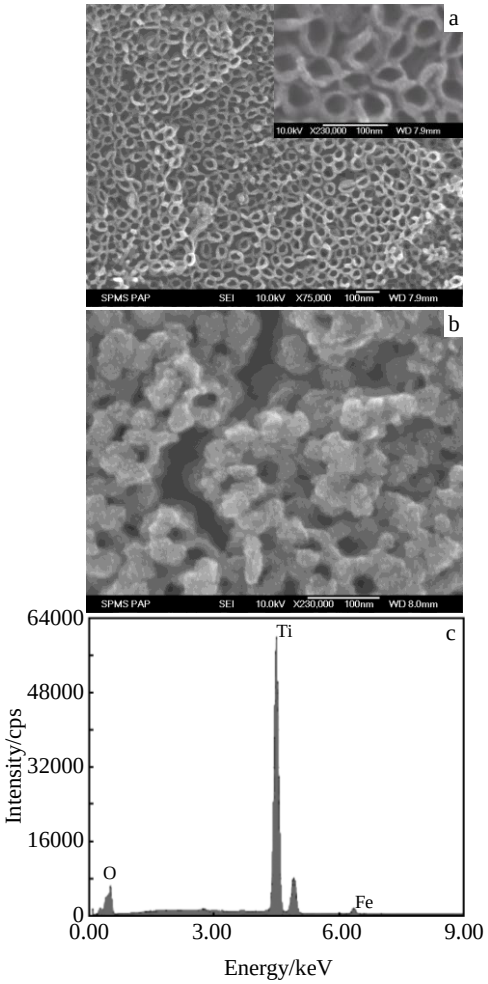

Fig.2 FESEM and EDS of the γ-Fe_2O_3/$TiO_{2\,(NT)}$ MHPs: (a) TiO_2 nanotubes, (b) γ-Fe_2O_3/$TiO_{2\,(NT)}$ MHPs, and (c) EDS spectrum

Only O, Fe and Ti elements can be detected using the energy dispersive spectroscopy (EDS) analysis, as shown in Fig.2c. The average atomic ratio of Fe to Ti elements is about 1:22, which agrees with that of the quantitative calculation by XRD.

2.3 Magnetic properties

γ-Fe_2O_3 is a 3d transition metal compound, where Fe^{3+} ions occupy interstices of a face-centered cubic closed packed frame of oxygen ions. The special structure leads to its magnetic properties. Fig.3 shows the field dependence of magnetization for MHPs measured at room temperature.

Significant hysteresis loops in the M-H curve indicate the superparamagnetic behavior of the γ-Fe_2O_3/$TiO_{2\,(NT)}$ MHPs and soft ferromagnetic behavior of the Fe_3O_4/$TiO_{2\,(NT)}$ MHPs. Superparamagnetism is the responsiveness to an applied magnetic field without retaining any magnetism after removal of the applied magnetic field. The saturation magnetization (M_s) for the γ-Fe_2O_3/$TiO_{2\,(NT)}$ MHPs is 1.32 A m^2 kg^{-1}, whereas that for the Fe_3O_4/$TiO_{2\,(NT)}$ MHPs is 2.45 A m^2 kg^{-1}. The

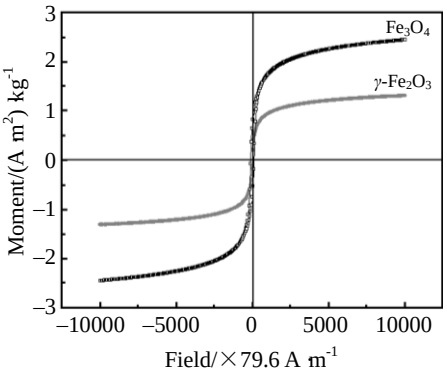

Fig.3 Magnetization hysteresis loops measured at room temperature

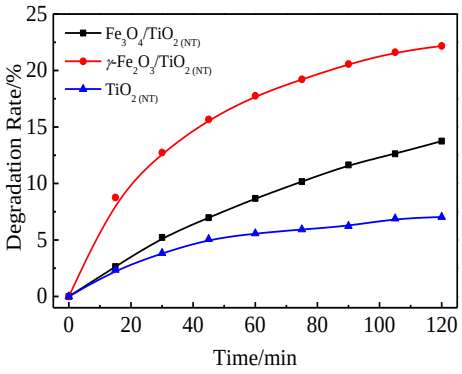

Fig.4 Degradation rate of MHPs as a function of degrading time

higher M_s of $Fe_3O_4/TiO_{2\,(NT)}$ MHPs is attributed to the stronger magnetization of Fe_3O_4 than that of γ-Fe_2O_3 in the heterojunction. The sample contains 5% γ-Fe_2O_3, thereby providing a value of 26.4 A m^2 kg^{-1}. The M_s is much lower than that of the corresponding bulk γ-Fe_2O_3 (74 A m^2 kg^{-1})[21], which may be due to the small size of the γ-Fe_2O_3 nanoparticles. This viewpoint has also been verified in the Ref. [22]. The result of *M-H* curve measurements indicate that the superparamagnetic property of MHPs is attributed to the γ-Fe_2O_3 nanoparticles.

2.4 Photocatalytic activity

The photocatalytic activities of γ-$Fe_2O_3/TiO_{2\,(NT)}$ and $Fe_3O_4/TiO_{2\,(NT)}$ MHPs were studied by degrading MB in a modulated wastewater; the results are shown in Fig.4. The MB is degraded at different levels under the action of the photocatalysts with sunlight irradiation; however, the photocatalytic activity of γ-$Fe_2O_3/TiO_{2\,(NT)}$ MHPs is significantly larger than those of $Fe_3O_4/TiO_{2\,(NT)}$ MHPs and pure TiO_2 nanotubes. Slightly higher photocatalytic activity of $Fe_3O_4/TiO_{2\,(NT)}$ MHPs than that of pure $TiO_{2\,(NT)}$ is also observed, which is not in agreement with that of Fe_3O_4/TiO_2 core/shell heterostructure [12]. The difference is mainly attributed to their different structure configurations. In the case of heterojunction arrays where some of the iron oxides (γ-Fe_2O_3 or Fe_3O_4) are exposed to the surface, any transferred charge carriers may still take part in subsequent redox reactions with either oxidants or reductants in the solution. These results indicate that the as-prepared γ-$Fe_2O_3/TiO_{2\,(NT)}$ MHPs possess significant photocatalytic activity.

Fe^{3+} can serve as a good electron capture agent because replacing Ti^{4+} with Fe^{3+} improves the capability of capturing electric load flow, prolongs the life of the e^-/h^+ pairs, and increases the photocatalytic activity. Moreover, the electron captured by Fe^{3+} can easily transfer to the Ti^{4+} surface. Electrical current load-transfer reaction is a slow process (nearly to 1 s), and interfacial charge transfer occurs in milliseconds. The e^-/h^+ pairs can easily coexist or be very close to the interface because of the lack of bond belt bending, causing the electrons to transmit easily and improve photocatalytic activity[23].

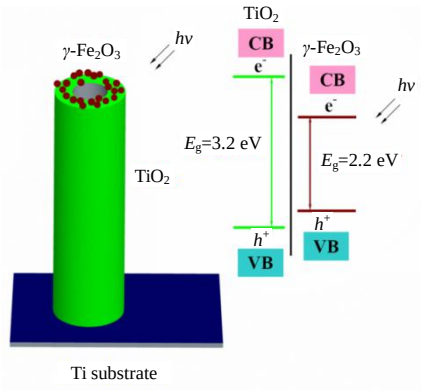

Fig.5 Sketch map of photocatalytic process for the γ-$Fe_2O_3/TiO_{2\,(NT)}$ MHPs under sunlight irradiation

The interaction between γ-Fe_2O_3 and TiO_2 evidently improves the charge separation and extends the TiO_2 response into the visible region. The possible charge separation process is schematically described in Fig.5. Upon visible absorption by γ-Fe_2O_3, the excited electrons from the γ-Fe_2O_3 nanoparticles could be quickly transferred to the TiO_2 nanotube arrays. Moreover, the formed heterojunction between γ-Fe_2O_3 and TiO_2 could further prevent the recombination between photoelectrons and holes. These well-separated photoelectrons and holes could participate in redox reaction, thereby enhancing the overall quantum efficiency. Fe_3O_4 can also produce more photoelectrons; however, the E_g of Fe_3O_4 is only 0.1 eV, indicating that it will be rapidly recombined and reduces the photocatalytic activity. The formed γ-$Fe_2O_3/TiO_{2\,(NT)}$ heterojunction arrays exhibit remarkable visible-light photocatalytic activity.

3 Conclusions

1) MHPs are provided with highly ordered TiO_2 nanotube arrays (55 nm in diameter and approximately 10 nm wall thickness) and with nano γ-Fe_2O_3 particle (approximately 15 nm) co-deposition.

2) MHPs present a superparamagnetic behavior of

γ-Fe_2O_3/$TiO_{2\,(NT)}$ MHPs and a soft ferromagnetic behavior of Fe_3O_4/$TiO_{2\,(NT)}$ MHPs.

3) The photocatalytic activity of γ-Fe_2O_3/$TiO_{2\,(NT)}$ MHPs is significantly larger than those of Fe_3O_4/$TiO_{2\,(NT)}$ MHPs or pure $TiO_{2\,(NT)}$ under visible light irradiation.

4) The interaction between γ-Fe_2O_3 and TiO_2 improves the charge separation and extends the TiO_2 response into the visible region. Moreover, the heterojunction between γ-Fe_2O_3 and TiO_2 could further prevent the recombination between photoelectrons and holes.

References

1 Hoffmann M R, Martin S T, Choi W Y *et al*. *Chemical Reviews* [J], 1995, 95: 69

2 Mozia S, Morawski A W, Toyoda M *et al*. *Desalination* [J], 2009, 241: 97

3 Wilke K, Breuer H D. *Journal of Photochemistry and Photobiology: A-Chemistry*[J], 1999, 121: 49

4 Mishra P R, Srivastava O N. *Bulletin of Materials Science*[J], 2008, 31: 545

5 Li G Z, Tang H P, Zhang W Y *et al*. *Rare Metal Materials and Engineering* [J], 2013, 42(11): 2341 (in Chinese)

6 Liang Y Q, Cui Z D, Zhu S L *et al*. *Electrochimica Acta*[J], 2010, 55: 5245

7 Kang T S, Smith A P, Taylor B E *et al*. *Nano Letters*[J], 2009, 9: 601

8 Yang B C, Uchida M, Kim H M *et al*. *Biomaterials*[J], 2004, 25: 1003

9 Paulose M, Varghese O K, Mor G K *et al*. *Nanotechnology*[J], 2006, 17: 398

10 Huang L H, Wang H J, Liu Y L *et al*. *Rare Metal Materials and Engineering* [J], 2011, 40(11): 1901 (in Chinese)

11 Xu J J, Ao Y H, Fu D G *et al*. *Journal of Physics and Chemistry of Solids* [J], 2008, 69: 1980

12 Beydoun D, Amal R, Low G K C *et al*. *Journal of Physical Chemistry B* [J], 2000, 104: 4387

13 Chen J Y, Qian Y X, Wei X Z. *Journal of Materials Science* [J], 2010, 45: 6018

14 Yu H, Chen S, Quan X *et al*. *Environmental Science & Technology* [J], 2008, 42: 3791

15 Paulose M, Mor G K, Varghese O K *et al*. *Journal of Photochemistry and Photobiology: A-Chemistry* [J], 2006, 178: 8

16 Anandan S, Ikuma Y, Niwa K. *Solid State Phenomena*[J], 2010, 162: 239

17 Soroka I L, Rooth M, Lu J *et al*. *Journal of Applied Physics*[J], 2009, 106: 084 313

18 Wu W, Xiao X H, Zhang S F *et al*. *Journal of Physical Chemistry C* [J], 2010, 114: 16 092

19 Xuan S H, Jiang W Q, Gong X L *et al*. *Journal of Physical Chemistry C* [J], 2009, 113: 553

20 Cullity B D, Stock S R. *Elements of X-Ray Diffraction*[M]. New Jersey: Prentice-Hall, Upper Saddle River, 2001: 402

21 delMonte F, Morales M P, Levy D *et al*. *Langmuir*[J], 1997, 13: 3627

22 Zhang L, Papaefthymiou G C, Ying J Y. *Journal of Physical Chemistry B* [J], 2001, 105: 7414

23 Shrestha N K, Macak J M, Schmidt-Stein F *et al*. *Angewandte Chemie-International Edition*[J], 2009, 48: 969

基于可见光磁性纳米 γ-Fe_2O_3/TiO_2 纳米管复合光催化剂

周广宏[1,2]，丁红燕[1]，朱雨富[1]，林岳宾[1]，刘　鹏[2]

(1. 淮阴工学院 江苏省介入医疗器械研究重点实验室，江苏 淮安 223003)

(2. 南洋理工大学数理学院，新加坡 637371)

摘　要：研究了基于可见光的磁性复合光催化剂纳米 γ-Fe_2O_3/$TiO_{2\,(NT)}$异质结阵列的制备方法，还研究了磁性复合光催化剂的表面形貌、微观结构、磁性能及其对亚甲基蓝的催化降解活性作用。结果表明，磁性复合光催化剂中的 TiO_2 纳米管阵列呈高度有序，其直径约 55 nm、壁厚约 10 nm，沉积在上面的 γ-Fe_2O_3 颗粒粒径约 15 nm。复合光催化剂 MHP 呈超顺磁性，其超顺磁性来源于 γ-Fe_2O_3 的小尺寸效应。在可见光的照射下 γ-Fe_2O_3/$TiO_{2\,(NT)}$的光催化性能明显大于 Fe_3O_4/$TiO_{2\,(NT)}$或纯 $TiO_{2(NT)}$。γ-Fe_2O_3 和 $TiO_{2\,(NT)}$之间的相互作用有利于电荷分离，并将 $TiO_{2(NT)}$红移至可见光区。此外，γ-Fe_2O_3 和 $TiO_{2\,(NT)}$之间所形成的异质结结构有利于阻止光电子和空穴之间的复合。

关键词：可见光；光催化；纳米管；异质结阵列；磁性

作者简介：周广宏，男，1970 年生，博士，淮阴工学院江苏省介入医疗器械研究重点实验室，江苏 淮安 223003，电话：0517-83559150，E-mail: zgh@hyit.edu.cn